18

Fuzzy-based kernel regression approaches for free form deformation and elastic registration of medical images

Edoardo Ardizzone, Roberto Gallea, Orazio Gambino and Roberto Pirrone
DINFO – Dipartimento di Ingegneria Informatica - Università degli Studi di Palermo
Italy

1. Introduction

In modern medicine, a largely diffused method for gathering knowledge about organs and tissues is obtained by means of merging information from several datasets. Such data are provided from multimodal or sequential acquisitions. As a consequence, a pre-processing step that is called "image registration" is required to achieve data integration.
Image registration aims to obtain the best possible spatial correspondence between misaligned datasets. This procedure is also useful to correct distortions induced by magnetic interferences with the acquisition equipment signals or the ones due patient's involuntary movements such as heartbeat or breathing.
The problem can be regarded as finding the transformation, generally defined by a set of parameters, that best maps one dataset (namely the input or floating image) onto the other (namely the target or base image). At the end of the process, corresponding pixels/voxels will have the same positions in both images/volumes.
This chapter starts presenting a brief taxonomy of literature registration methods. Then, an excursus of novel registration methods is presented after a more detailed explanation of the Thin-Plate Spline approach (Bookstein, 1989), which is a milestone in the field. All of these schemes use a "fuzzy kernel-based" approach able to cope with many types of deformations. The described procedures are examples of landmark-based approaches that rely on a set of a priori known control points, even though the same concepts could be extended to area-based approaches where no control points need to be detected.
All of the methods use fuzzy membership maps in a probabilistic discriminative model, which is based on kernel regression. Such techniques are based on concepts derived by Fuzzy c-means clustering process (Dunn, 1973 and Bezdek, 1981). However, no clustering algorithm needs to be performed at all.
The framework uses several measures, both quantitative and qualitative to evaluate the performance of the method.
In all of the presented approaches the global mapping function is recovered as a continuous and smooth composition of local mappings. This philosophy allows dealing with subtle local deformations without the need of using extremely time consuming complex models.

The methods were extensively tested and validated and the experimental results are reported. Final considerations and future work are then discussed.

2. Methods for image registration

Even though image registration is used for a large variety of applicative contexts, applications can be divided in four categories, depending on the image acquisition strategy:

- *Different viewpoints (or multi-view analysis)*: The same object or scene is acquired from different viewpoints: the goal is to obtain a larger view or a 3d representation of the object.
- *Different times (or multi-temporal analysis)*: Images of the same object are acquired in different times, perhaps under different conditions. The aim is to evaluate differences between two or more acquisitions.
- *Different sensors (or multimodal analysis)*: Images of the same object are acquired by different sensors, for example magnetic resonance (MR), computer tomography (CT), positron emission tomography (PET), etc.
- *Scene to model registration*: images of a real scene and its model are registered. The model can be a synthetic representation or another scene with similar content. The purpose of this method is to find the acquired image in the model and compare them.

Since there exists a lot of image types, it is impossible to design a universal method suitable for all application purposes. Each method should take into account the objects to be registered and the characteristics of the deformations to be recovered. Furthermore, even more elements such as noise corruption should be considered too. Generally, a distinction between *feature-based* and *area-based* approaches is operated, depending on how much information is used for the registration task, in the first case just a sparse information subset (the features) is used for recovering the mapping, in the latter all of the images information is taken into account. Nonetheless, every strategy generally uses four steps, with the exception of the first one. These steps are the following:

- *Feature detection*: salient and unambiguous objects such as corners, intersections, contours, etc., are manually or automatically detected in both the input and reference image. This step is omitted in area-based strategies.
- *Feature matching*: the correspondences between the images are found by means of matching the previously detected features. For this purpose, there exist several feature descriptors and similarity measures based on features appearance or informative content. Since area-based strategies use all of the image information; such methods use a dense features map simply defined by all of the pixels/voxels in the images.
- *Transform model estimation*: after the features are matched, this information is used to recover a transformation function, which defines the deformation needed to map every pixel/voxel of the input image onto every pixel/voxel of the reference image. Such a function is determined by choosing its type and defining the value of its set of parameters.
- *Image resampling and transformation*: once the deformation estimation is achieved, the mapping function is applied on the input image. Since this mapping generally brings the pixels/voxels in non-integer coordinates, proper interpolation techniques need to be used in order to avoid or limit resampling artefacts.

Each of the steps has its intrinsic problems, so each of them has to be developed taking into account the properties of the objects that have to be registered. For example the presence of noise can affect feature detection. So, if noise is assumed to be present, the detection procedure should be robust. A potential problem in feature matching is the different appearance of corresponding features due to illumination conditions or to sensors spectral sensitivity; in this case the similarity measure adopted needs to take into account these factors.
In literature there exists a large variety of approaches that had been used to deal with the registration problem. As mentioned, there not exist a unique solution since each one has its specific applicative context. Global mapping models use bivariate low-degree polynomials as mapping function. This strategy is often not suited for real cases due to the presence of local deformations in the images; however, it is used frequently as a starting point for other methods. Local mapping models overcome these limitations by registering locally the different areas of the image. Radial basis functions such as Thin-Plate spline (Bookstein, 1989) or Wendland's functions (Wendland 1995, Fornefett et al. 1999) are also used, and they are able to deal with local deformations, even if they could be considered as global mapping models. Another approach, which does not require the use of any parametric function is to model complex deformations by considering the image as a tensile material (Bajcsy R. and Kovacic S., 1989) or a viscous fluid (Bro-Nielsen and Gramkow, 1996) deformed by external and internal forces subject to constraints. Registration is achieved by the iterative minimization of an energy functional.

2.1 A classical approach: the Thin Plate Spline

One of the classical approaches to image registration is the Thin Plate Spline (TPS). The name is derived from the physical analogy, which involves the bending of a thin metal sheet. In the context of spatial coordinates transformation and image registration, lifting the plate corresponds to displace the image in one direction (i.e. *x, y* or *z* axis). The Thin Plate Spline is a parametric interpolation function which is defined by *D(K+3)* parameters, where *D* is the number of spatial dimensions of the datasets and *K* is the number of the given landmark points where the displacement values are known. The function is a composition of an affine part, defined by *3* parameters, and *K* radial basis functions, defined by an equal number of parameters. In 2d its analytic form is defined as:

$$g\left(\mathbf{p}\right) = ax + by + d + \sum_{i=1}^{K} \rho\left(\left\|\mathbf{p} - \mathbf{c_i}\right\|^2\right) w_i; \qquad \mathbf{p} = \begin{bmatrix} x \\ y \end{bmatrix}; \qquad \mathbf{c_i} = \begin{bmatrix} c_x \\ c_y \end{bmatrix}, \tag{1}$$

where $\mathbf{p}$ is the input point, $\mathbf{c_i}$ are the landmark points and the radial basis function $\rho(r)$ is given by:

$$\rho(r) = \frac{1}{2} r^2 \log r^2, \tag{2}$$

All of the TPS parameters are computed solving a linear system defined by a closed-form minimization of the bending energy functional. Such functional is given by:

$$E_{tps} = \sum_{i=1}^{K} \left\| y_i - g\left(\mathbf{p}_i\right) \right\| + \lambda \iint \left[\left(\frac{\partial^2 g}{\partial x^2} \right)^2 + 2\left(\frac{\partial^2 g}{\partial xy} \right)^2 + \left(\frac{\partial^2 g}{\partial y^2} \right)^2 \right] dxdy. \tag{3}$$

The functional is composed by two terms: the data term and the regularization term. The former minimizes the difference between known and recovered displacements at landmark points, the latter minimizes the bending energy of the recovered function, i.e. maximises its smoothness and it is weighted by the parameter λ. As mentioned before, for this expression a closed-form analytical solution exists, from which is possible to recover all of the required spline function parameters. The main characteristic of this function is that it exhibits minimum curvature properties.

3. Registration with fuzzy-based kernel regression

In our study we developed a class of registration algorithms, which exploit kernel regression model to recover the mapping functions. The classic kernel regression is enhanced by fuzzy related techniques, in particular the C-means clustering algorithm.
The registration schemes proposed are similar as regards the theoretical concepts they rely on, while they differ in their application. Two strategies are discussed: the former is a simple landmark-based registration approach (Ardizzone et al., 2009-1) that is described to explain how the fuzzy kernel regression concepts can be applied to elastic registration. In this scheme the global transformation function is recovered directly from the landmarks displacements. The latter strategy (Ardizzone et al., 2009-2) differs from the previous one in that the regression is used to obtain a smooth composition of affine transformations recovered from the triangulation of landmark points. Both techniques do not need to perform neither iterative nor analytic minimization procedures.

3.1 Kernel regression

In pattern recognition, there exists a class of techniques, which uses data points or a subset of them not just in the training phase, but also in the prediction phase. These are called *memory-based* methods. Linear parametric models that can be re-cast into equivalent dual representations where the predictions are given by linear combinations of a *kernel function* evaluated at the training data points are known as kernel regression methods. Kernel functions are symmetric in their argument and are defined by training data points. Kernels, which depend only on the magnitude of the distance of the argument from the training points, are known as *homogeneous* kernels or *radial basis functions*.
For our registration purpose we will use the derivation of kernel regression from the scheme known as the Nadaraya-Watson model (Nadaraya, 1964 and Watson, 1964). Assuming we have a training set $\{x_n, t_n\}$. Then, using a Parzen density estimator, the joint distribution $p(x, t)$ is modeled as

$$p(x,t)=\frac{1}{N}\sum_{n=1}^{N} f(x-x_n,t-t_n) \tag{4}$$

where *f(x, t)* is the component density function, and there is a component centered on each data point. The regression function *y(x)*, corresponding to the conditional average of the target variable conditioned on the input variable, is given by:

$$y(x)=E[t\mid x]=\int_{-\infty}^{+\infty} tp(t\mid x)dt=\frac{\int tp(x,t)dt}{\int p(x,t)dt}= \\ =\frac{\sum_n \int tf(x-x_n,t-t_n)dt}{\sum_m \int f(x-x_m,t-t_m)dt} \tag{5}$$

Assuming that the component density functions have zero mean so that

$$\int_{-\infty}^{+\infty} f(x,t)dt=0 \tag{6}$$

for all values of *x*, then, operating a change of variable we get

$$y(x)=\frac{\sum_n g(x-x_n)t_n}{\sum_m g(x-x_m)}=\sum_n k(x,x_n)t_n \tag{7}$$

where the kernel function $k(x, x_n)$ is defined as

$$k(x,x_n)=\frac{g(x-x_n)}{\sum_m g(x-x_m)} \tag{8}$$

and

$$g(x)=\int_{-\infty}^{+\infty} f(x,t)dt \tag{9}$$

This form (7) represents the *Nadaraya-Watson* model, for localized kernel function. It has the property of weighting more the data points x_n close to *x* than the other ones. The kernel (8) satisfies the summation constraint

$$\sum_{n=1}^{N} k(x, x_n) = 1 \tag{10}$$

This result points out that the prediction for the value of a data point x is given by a linear combination of the training data points values and the kernel functions. Such kernel functions can have different forms, provided that (10) is satisfied.

3.2 Fuzzy c-means

Before explaining how kernel regression can be applied to the registration task, it is necessary to describe the Fuzzy c-means clustering technique (Bezdek, 1981) that is a powerful and efficient data clustering method.

Each data sample, represented by some feature values in a suitable space, is associated to each cluster by assigning a membership degree. Each cluster is identified by its centroid, a special point where the feature values are representative for its own class. The original algorithm is based on the minimization of the following objective function:

$$J_S = \sum_{j=1}^{m} \sum_{i=1}^{k} \left(u_{ij}\right)^s d\left(x_i, c_j\right)^2, \qquad 1 \le s \le \infty \tag{11}$$

where $d(x_i, c_j)$ is a distance function between each observation vector x_j and the cluster centroid c_j, s is a parameter which determines the amount of clustering fuzziness, m is the number of clusters, which should be chosen a priori, k is the number of observations and u_{ij} is the membership degree of the sample x_i belonging to cluster centroid c_j.

An additional constraint is that the membership degrees should be positive and structured such that $u_{i1} + u_{i2} + ... + u_{im} = 1$. The method advances as an iterative procedure where, given the membership matrix $U = [u_{ij}]$ of size k by m, the new positions of the centroids are updated as:

$$c_j = \frac{\sum_{i=1}^{k} \left(u_{ij}\right)^s x_i}{\sum_{i=1}^{k} \left(u_{ij}\right)^s} \tag{12}$$

The algorithm ends after a fixed number of iterations or when the overall variation of the centroids displacements over a single iteration falls below a given threshold. The new membership values are given by the following equation:

$$u_{ij} = \frac{1}{\sum_{l=1}^{m} \left(\frac{d\left(x_i, c_j\right)}{d\left(x_i, c_l\right)} \right)^{\frac{2}{s-1}}} \tag{13}$$

To better understand the whole process a one-dimensional example is reported (i.e. each data point is represented by just one value).
Twenty random data points and three clusters are used to initialize the procedure and compute the initial matrix U. Note that the cluster starting positions, represented by vertical lines), are randomly chosen. Fig. 1 shows the membership values for each data point relative to each cluster; their colour is assigned on the basis of the closest cluster to the data point.

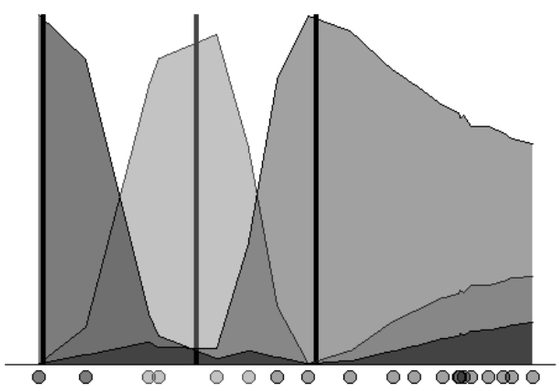

Fig. 1. Fuzzy C-means example: initial membership value assignation.

After running the algorithm, the minimization is performed and the cluster centroids are shifted, the final membership matrix U can be computed. The resulting membership functions are depicted in Fig. 2

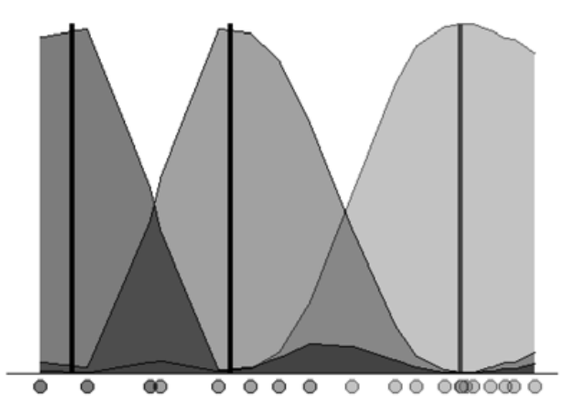

Fig. 2. Fuzzy C-means example: final membership value assignation and cluster centres positions.

3.3 Fuzzy kernel regression

Merging the results of the previous discussion it turns out that Fuzzy C-means membership functions can be used as kernels for regression in the Nadaraya-Watson model because they

satisfy the summation constraint. In the scenario of image registration, the input variables populate the feature space by means of the spatial coordinates of the pixels/voxels and cluster centroids are represented by relevant points in the images, whose spatial displacement is known. The landmark points where correspondences are known between input and reference image can be used for this purpose.
As a result of such setting there is no need to execute any minimization of the Bezdek functional, since image points are already supposed to be clustered around the landmark points (or equivalent representative points). Fuzzy C-means is used just as a starting point for the registration procedure. Once the relevant points are known, a single FCM step is performed to construct Fuzzy kernels by means of computing membership functions. For this purpose the distance measure used in (13) is the simple Euclidean distance, since just spatial closeness is required to determine how much any point is influenced by surrounding relevant points. Such membership functions are then used to recover the displacement for any pixel/voxel in the image using the following formula:

$$y(x) = \sum_n u(x, x_n) t_n \tag{14}$$

where $u(x,x_n)$ is the membership value for the current pixel/voxel with regard to the relevant point x_n, and t_n is a 2d/3d vector or function representing its known xy or xyz displacement. This will result in continuous and smooth displacement surfaces, which interpolate relevant points.
Even if the registration framework is unique, it can be applied in several ways, depending on the choice of the target variable, i.e. what is assumed to be the prior information in terms of relevant points and their known displacement. In the following paragraphs two different applications of the proposed framework will be described.

3.4 Simple landmark based elastic registration

A first application arises naturally from the described framework. It is very simple and is meant to demonstrate the actual use of the fuzzy kernel regression. However since it is effective notwithstanding its simplicity, it could be used for actual registration tasks.
Basically, it consists in considering the landmark points themselves directly as the relevant points representing the cluster centroids for the FCM step, and their displacements vectors directly as the target variables. Each pixel/voxel is then subjected to a displacement contribute from each landmark point. Such contribute is high for closer points and gets smaller while relative distances between the input points and the landmarks increase. The final displacement vector for any input point will consequently be a weighted sum of the landmarks points.
To better understand this technique an example of the procedure is explained: a pattern image showing four landmark points is depicted in Fig. 3a. An input point P is considered, and its distances from the four landmarks are shown. After the procedure is applied with a fuzziness value s set to 1.6, the point P results to have the following membership values for the four landmarks:

$$u_{ij} = [0.0371, 0.0106, 0.9339, 0.0183] \tag{15}$$

This means that it will receive the greatest part of the displacement contribute from the bottom-left landmark, and just a marginal contribute from the other three. The results are confirmed in Fig. 3b, where the point has been moved according to a displacement vector that is mostly similar to the displacement of the third landmark. Anyway, other landmarks give small influences too.

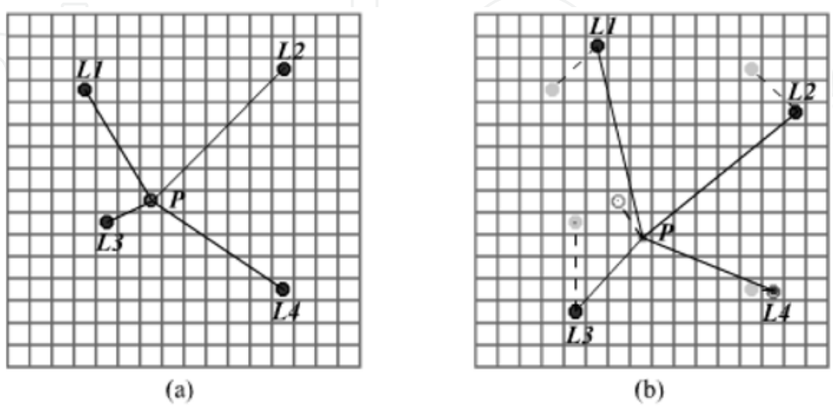

Fig. 3. Example of single point registration using four landmarks.

Repeating the same procedure for the points in the whole image, complete dense displacement surfaces are recovered, one for each spatial dimension. Such surfaces have continuity and smoothness properties.
As a first example, visual results for conventional images are shown in Fig. 4.

Fig. 4. Example of registration of conventional images. Input image (a), registered image (b) and target image (c). In this example 31 landmark points were used with the fuzziness s value set to 1.6

In Fig. 5 are shown the recovered displacement surfaces for x (a) and y (b) values respectively.

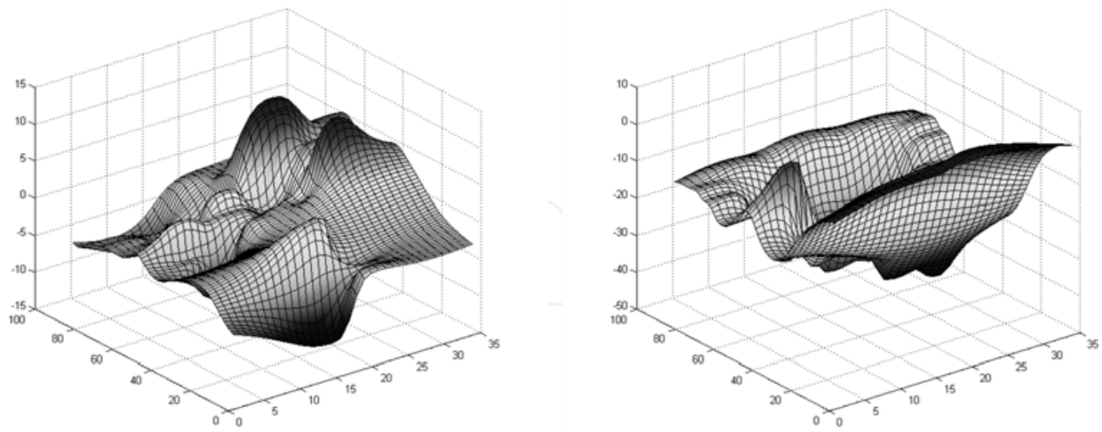

(a) (b)

Fig. 5. Displacement surfaces recovered for x (a) and y (b) values.

3.5 Improved landmarks based elastic registration

Although the simple method previously described is effective and can be useful for simple registration tasks, it does not result suitable for many applications in that it does not take properly into account relations between neighbouring landmark points. In other words, considering a single point displacement vector to represent the deformation of the image in different areas is not enough. Thus, it is necessary to find an effective way for estimating such zones. Given some landmark points, a simple way to subdivide the image space in regions is the application of the classic Delaunay triangulation procedure (Delaunay, 1934), which is the optimal way of recovering a tessellation of triangles, starting from a set of vertices. It is optimal in the sense that it maximizes the minimum angle among all of the triangles in the generated triangulation. Starting from the landmark points and their correspondences, such triangulation produces a most useful triangles set along their relative vertices correspondences. An example of Delaunay triangulation is depicted in Fig. 6.

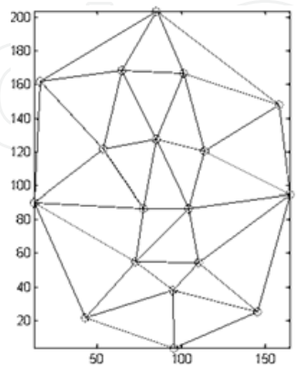

Fig. 6. Example of Delaunay triangulation.

Once we have such triangle tessellation whose vertices are known as well as their displacements, it is possible to recover the local transformations, which map each triangle of the input image onto its respective counterpart in the target image. Such transformation can be recovered in several ways; basically an affine transformation can be used. In 2d space affine transforms are determined by six parameters. Writing down the transformation equation (16) for three points a linear system of six equations to recover such parameters can be obtained. Similar considerations hold for the three-dimensional case.

$$\begin{bmatrix} x \\ y \\ 1 \end{bmatrix} = \begin{bmatrix} a & b & c \\ d & e & f \\ 0 & 0 & 1 \end{bmatrix} \begin{bmatrix} x_{0,n} \\ y_{0,n} \\ 1 \end{bmatrix} = \begin{bmatrix} ax_0 + by_0 + c \\ dx_0 + ey_0 + f \\ 1 \end{bmatrix} \Rightarrow \begin{cases} x_1 = ax_{0,1} + by_{0,1} + c \\ y_1 = dx_{0,1} + ey_{0,1} + f \\ x_2 = ax_{0,2} + by_{0,2} + c \\ y_2 = dx_{0,2} + ey_{0,2} + f \\ x_3 = ax_{0,3} + by_{0,3} + c \\ y_3 = dx_{0,3} + ey_{0,3} + f \end{cases} \tag{16}$$

Each transformation is recovered from a triangle pair correspondence, and the composition of all the transformations allows the full reconstruction of the image. Anyway, this direct composition it is not sufficient per se, since it presents crisp edges because transition between two different areas of the image are not smooth even if the recovered displacement surfaces are continuous due to the adjacency of the triangles edges. This can lead to severe artefacts in the registered image, especially for points outside of the convex hull defined by the control points (Fig. 7c and Fig. 7d), where no transformation information is determined. To better understand this problem an example of registration along the recovered surfaces plot are shown respectively in Fig. 7 and Fig. 8.

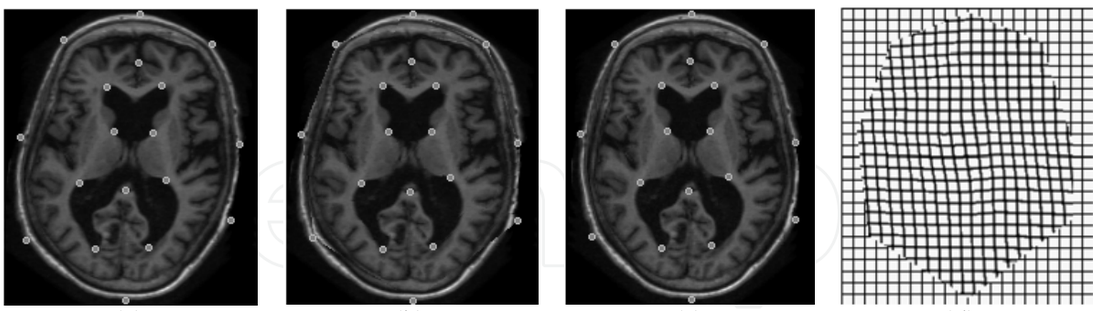

(a) (b) (c) (d)

Fig. 7. Example of MRI image registration with direct composition of affine transformations. Input image (a), registered image (b) and target image (c). Deformed grid in (d). In this example 18 landmark points were used.

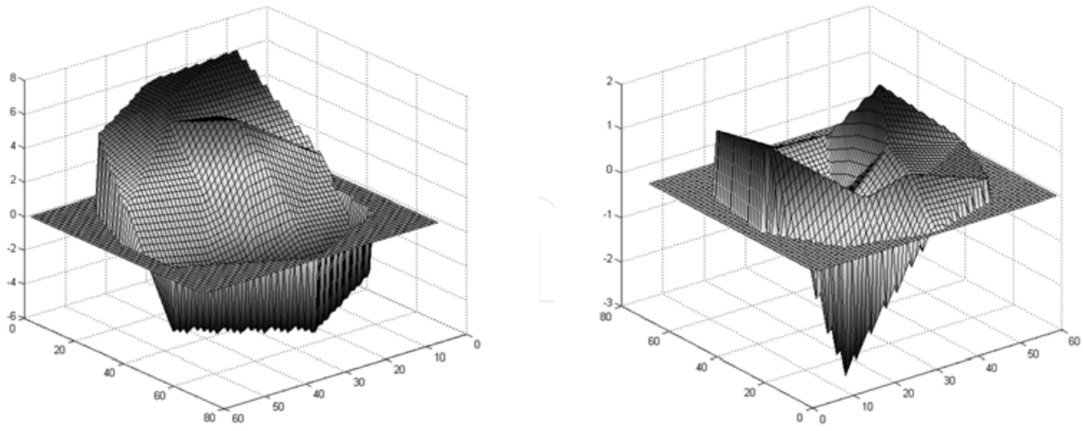

(a) (b)

Fig. 8. Displacement surfaces recovered for x (a) and y (b) values with direct affine transformation composition.

Fuzzy kernel regression technique can be used to overcome this drawback. To apply the method, relevant points acting as cluster centroids must be chosen. Since our prior displacement information is no more about landmark points, but about triangles, they cannot be chosen as relevant points anymore. Thus, we have to choose some other representative points for each triangle. For this purpose, centres of mass are used as relevant points, and their relative triangle affine transformation matrix is the target variable. In this way, after recovering the membership functions and using them as kernels for regression, final displacement for each pixel/voxel is given by the weighted sum of the displacements given by all of the affine matrices. In this way the whole image information is taken into account. The final location of each pixel/voxel is then obtained as follows (2d case):

$$\begin{bmatrix} x \\ y \\ 1 \end{bmatrix} = \sum_n \left(u_n(x,y) \begin{bmatrix} a_n & b_n & c_n \\ d_n & e_n & f_n \\ 0 & 0 & 1 \end{bmatrix} \begin{bmatrix} x_0 \\ y_0 \\ 1 \end{bmatrix} \right) \tag{17}$$

In this way there are no more displacement values that change sharply when crossing triangle edges, but variations are smooth according to the choice of the fuzziness parameter s. In Fig. 9. and Fig. 10 registration results and deformation surfaces for the previous examples are shown. Note that there are no more sharp edges in the surface plots and a displacement value is recovered also outside of the convex hull defined by the landmarks points.

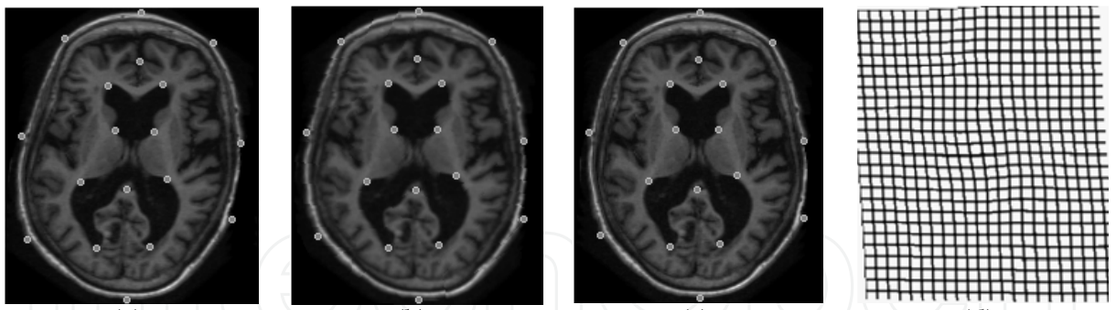

(a) (b) (c) (d)

Fig. 9. Example of MRI image registration with fuzzy kernel regression affine transformations composition. Input image (a), registered image (b) and target image (c). Deformed grid in (d). In this example 18 landmark points were used.

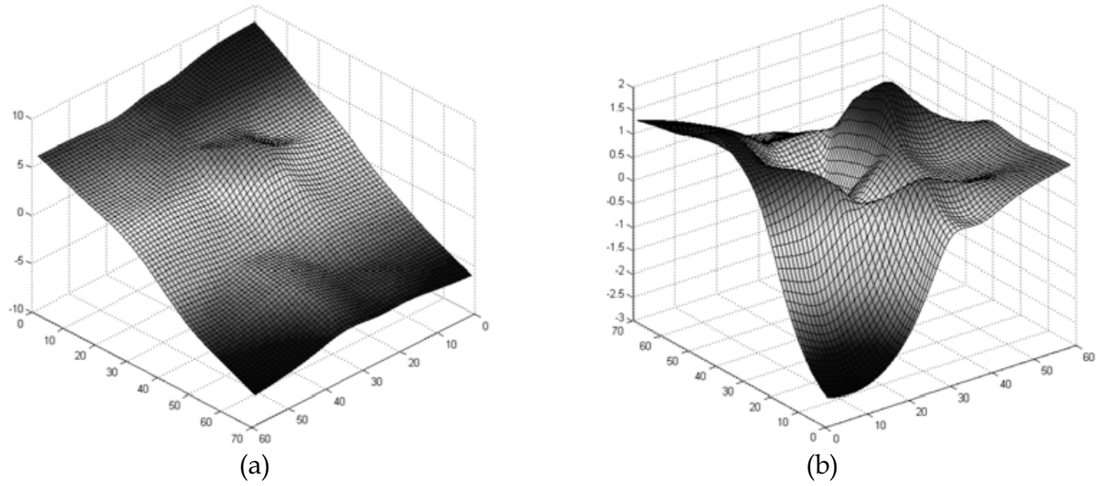

(a) (b)

Fig. 10. Displacement surfaces recovered for x (a) and y (b) values with fuzzy kernel regression affine transformation composition.

3.6 Image resampling and transformation

Once the mapping functions have been determined, the actual pixels/voxels transformation has to be realized. Such transformation can be operated in a forward or backward manner. In the forward or direct approach (Fig. 11a), each pixel of the input image can be directly transformed using the mapping function. This method presents a strong drawback, in that it can produce holes and/or overlaps in the output image due to discretization or rounding errors. With backward mapping (Fig. 11b), each point of the result image is mapped back onto the input image using the inverse of the transformation function. Such mapping generally produces non-integer pixel/voxel coordinates, so resampling via proper interpolation methods is necessary even though neither holes nor overlaps are produced.

Such interpolation is generally produced using a convolution of the image with an interpolation kernel.

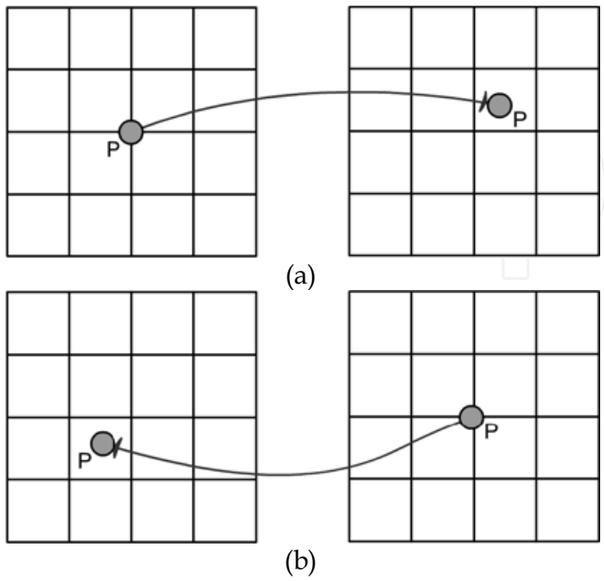

Fig. 11. Direct mapping (a) and inverse mapping (b).

The optimal interpolating kernel, the *sinc* function, is hard to implement due to its infinite support extent. Thus, several simpler kernels with limited support have been proposed in literature. Among them, some of most common are nearest neighbour (Fig. 12a), linear (Fig. 12b) and cubic (Fig. 12c) functions, Gaussians (Fig. 12d) and Hamming-windowed sinc (Fig. 12e). In Table 1 are reported the expressions for such interpolators.

Interpolating with the nearest neighbour technique consists in convolving the image with a rectangular window. Such operation is equivalent to apply a poor sinc-shaped low-pass filter in the frequency domain. In addition it causes the resampled image to be shifted with respect to the original image by an amount equal to the difference between the positions of the coordinate locations. This means that such interpolator is suitable neither for sub-pixel accuracy nor for large magnifications, since it just replicates pixels/voxels.

A slightly better interpolator is the linear kernel, which operates a good low-pass filtering in the frequency domain, even though causes the attenuation of the frequencies near the cut-off frequency, determining smoothing of the image. Similar, though better results are achieved using a Gaussian kernel.

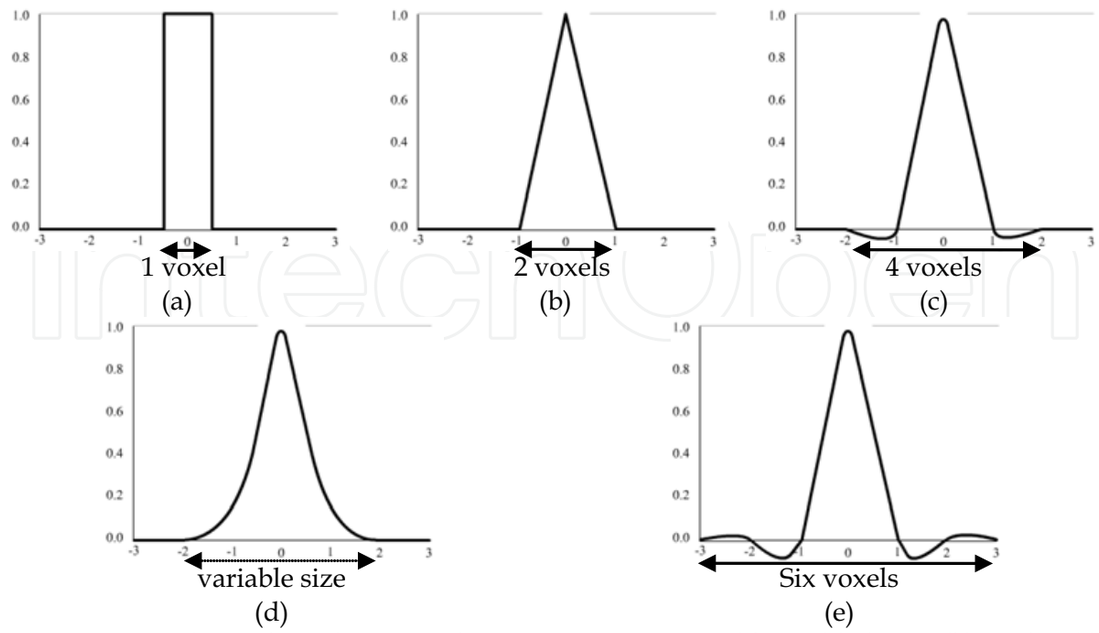

Fig. 12. Interpolation kernels in one dimension: nearest neighbour (a), linear (b), Cubic (c), Gaussian (d) and Hamming-windowed sinc (e). Width of the support is shown below (pixel/voxel number).

INTERPOLATOR	FORMULA FOR INTERPOLATED INTENSITY
Nearest Neighbour	$= \begin{cases} n_0 & if\ x < 0.5 \\ n_1 & otherwise \end{cases}$
Linear	$= (1-x)n_0 + xn_1$
Cubic Spline	$= \begin{cases} (a+2)x^3 - (a+3)x^2 + 1 & if\ 0 \le x \le 1 \\ ax^3 - 5ax^2 + 8ax - 4a & if\ 1 < x \le 2 \end{cases}$
Gaussian	$= \frac{1}{\sigma\sqrt{2\pi}} e^{\frac{(x-\mu)^2}{2\sigma^2}} \quad ;\sigma > 0$
Hamming-sinc	$= \sum_{i=-2}^{3} w_i n_i \Big/ \sum_{i=-2}^{3} w_i$ where $w_i = \left(0.54 + 0.46\cos\left(\frac{\pi(x-i)}{3}\right)\right)\left(\frac{\sin(\pi(x-i))}{\pi(x-i)}\right)$

Table 1. Analytic expression for several interpolators in one dimension.

Cubic Interpolator are generally obtained by means of spline functions, constrained to pass from points (0, 1), (1, 0) and (2,0), and to have continuity properties in 0 and 1; in addition the slope in 0 and 2 should be 0, and approaching 1 both form left and right, it must be the same. Since a cubic spline has eight degrees of freedom, using these seven constraints, the function is defined up to a constant *a*. Investigated choice of the *a* parameter are 1, -3/4, and 1/2 (Simon, 1975).
Due to the problems of using an ideal sinc function, several approximation schemes have been investigated. Direct truncation of the function is not possible because cutting the lobes generates the ringing phenomenon. A more performing alternative is to use a non-squared window, such as Hamming's raised cosine window.

4. Experimental results and discussion

Simple Fuzzy Regression (SFR) and Fuzzy Regression Affine Composition (FRAC) have been extensively tested with quantitative and qualitative criteria using both real and synthetic datasets (Cocosco et al., 1997, Kwan et al., 1996-1999, Collins et al., 1998). The first type of tests consists in the registration of a manually deformed image onto its original version. The test image is warped using a known transformation, which is recovered operating the registration. The method performance is then evaluated using several similarity metrics: sum of squared difference (SSD), mean squared error (MSE) and mutual information (MI) as objective measures, Structural Similarity (SSIM) as the subjective one (Wang et al., 2004). The algorithm was ran using different fuzziness values *s*, visual results for the proposed method are depicted in Fig. 13 and Fig. 14 and measures are summarized in Table 2 and Table 3. Comparisons with Thin-Plate Spline approach are also presented.

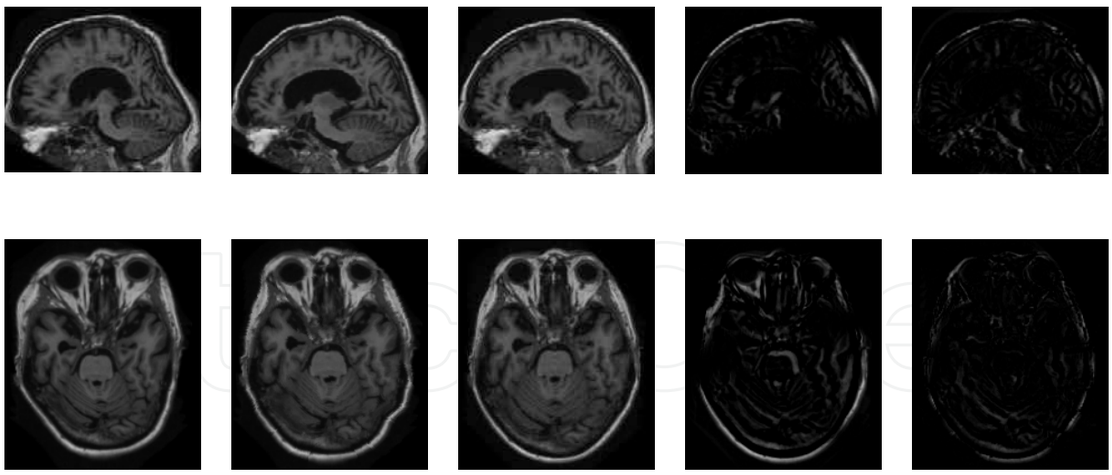

Fig. 13. Example of registration results with simple fuzzy kernel regression. From left to right: input image, registered image, target image, initial image difference, final image difference.

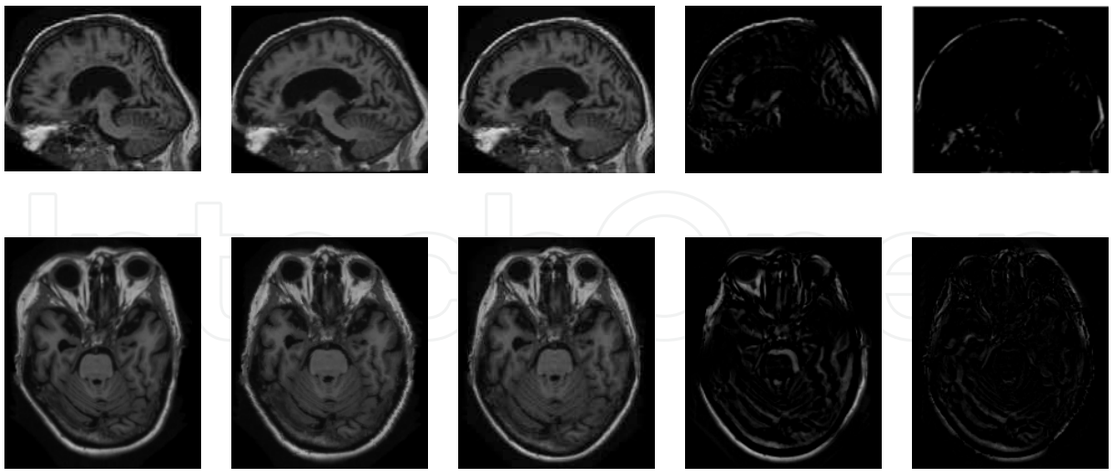

Fig. 14. Example of registration results with fuzzy kernel regression affine transformation composition. From left to right: input image, registered image, target image, initial image difference, final image difference.

	Simple Fuzzy Regression				Thin Plate Spline			
s	MSE	SSD	MI	SSIM	MSE	SSD	MI	SSIM
1.2	0.0287	1049	1.0570	0.6753				
1.4	0.0254	929	<u>1.0945</u>	<u>0.6893</u>				
1.6	<u>0.0251</u>	<u>917</u>	1.0519	0.6552				
1.8	0.0282	1033	1.0090	0.6225	0.0243	903	1.0856	0.6759
2.0	0.0361	1322	0.9563	0.5877				
2.2	0.0426	1560	0.8970	0.5534				
2.4	0.0486	1779	0.8489	0.5250				

Table 2. Comparison of similarity measures between Simple Fuzzy Regression and Thin Plate Spline approaches. Best results are underlined.

	Fuzzy Regression Affine Composition				Thin Plate Spline			
s	MSE	SSD	MI	SSIM	MSE	SSD	MI	SSIM
1.2	0.0112	410	1.1666	0.7389				
1.4	<u>0.0101</u>	<u>369</u>	1.1811	<u>0.7435</u>				
1.6	0.0111	408	<u>1.1834</u>	0.7385				
1.8	0.0133	486	1.1329	0.7037	0.0115	412	1.1654	0.7294
2.0	0.0201	736	1.0044	0.6257				
2.2	0.0277	1015	0.8985	0.5590				
2.4	0.0370	1355	0.8158	0.5115				

Table 3. Comparison of similarity measures between Fuzzy Regression Affine Composition and Thin Plate Spline approaches. Best results underlined.

From the previous tables it results that the obtained similarity measures are comparable to the Thin Plate Spline in the case of SFR registration, and better for FRAC Registration, so the proposed methods are a valid alternative from an effectiveness point of view.
From an efficiency perspective, different considerations hold. All of the tests were conducted on a AMD Phenom Quad-core running Matlab 7.5 on Windows XP. Timing performance exhibited a large speed up for both of the presented algorithms in respect of TPS: using 22 landmark points on 208x176 images, mean execution time for SFR registration is 30,32% of TPS, while for FRAC registration it is 49,65%. Such difference is due to the fact that TPS requires the solution of a linear system composed by an high number of equations, this task is not needed for the proposed methods which reduce just to distance measures and weighted sums for SFR and FRAC, the latter is a bit more expensive since the affine transformation parameters have to be recovered from simple six equations systems (2d case).
Last considerations are for memory consumption. Comparing the size of data structures, it can be seen that for SFR algorithm DxM values need to be stored for landmarks displacements, where D is the dimensionality of the images and M the number of control points, and M values are needed for the membership degrees of each point. However, once every single pixel/voxel has been transformed, its membership degrees can be dropped, so the total data structure is $M(D+1)$ large. TPS approximation has a little more compact structure, in fact it needs just to maintain the $D(M+3)$ surface coefficients (M for the non-linear part and 3 for the linear one). FRAC has the largest descriptor, it is variable since it depends on the number of triangles in which the image is subdivided, and anyway it is in the order of $2M$. Since each affine transformation is defined by $D(D+1)$ parameters and membership degrees require $2M$ additional values (i.e. one for each triangle) the whole registration function descriptor is in the order of $2M[D(D+1)+1]$. In conclusion, the storing complexity is $O(M)$ for both methods, i.e. linear in the number of landmarks used, and thus equivalent.

4.1 Choosing the *s* parameter

As resulted from the discussion of the registration methods, both techniques require the parameter s, the fuzziness value, to be assigned. Even though there exists the problem of tuning this term, experiments shown that each of the considered similarity measures is a convex (or concave) function of the s parameter and that the optimal value generally lies in 1.7 ± 0.3. Furthermore, in this range results are very similar. Anyway, if a fine-tuning is required, a few mono-dimensional search attempts (3-4 trials on average) are enough to find the optimum solution using bisectional strategies such as golden ratio thus keeping the method still more efficient than Thin Plane Spline.

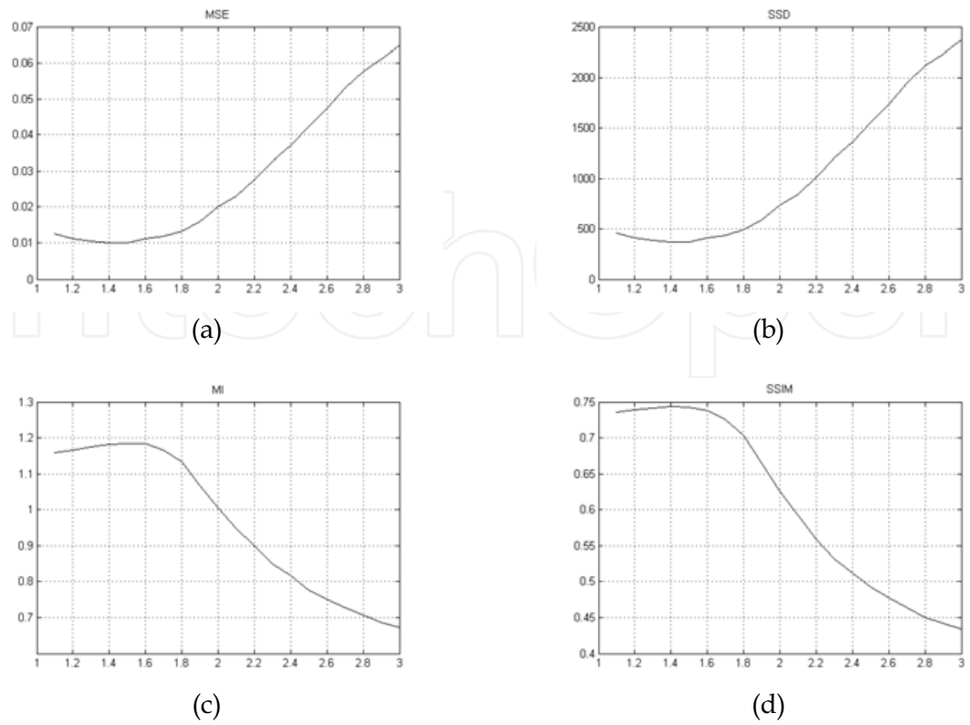

Fig. 15. Example of plot of the similarity measures versus the *s* parameters: MSE (a), SSD (b), MI (c) and SSIM (d).

4.2 Interpolation performance

The interpolation schemes described provide different visual results exhibiting different quality performances. Fig. 16 depicts the visual results achieved by the described interpolators. However, especially when dealing with 3d volumes, computational burden may be eccessive compared to the quality of the resampled images. Table 4 shows the average computational time normalized with respect to nearest neighbour performance.

INTERPOLATOR	TIMING PERFORMANCE
Nearest Neighbour	1
Linear	2.8534
Cubic Spline	4.1328
Gaussian	2.7913
Hamming-sinc	4.9586

Table 4. Timing performance for resampling kernels.

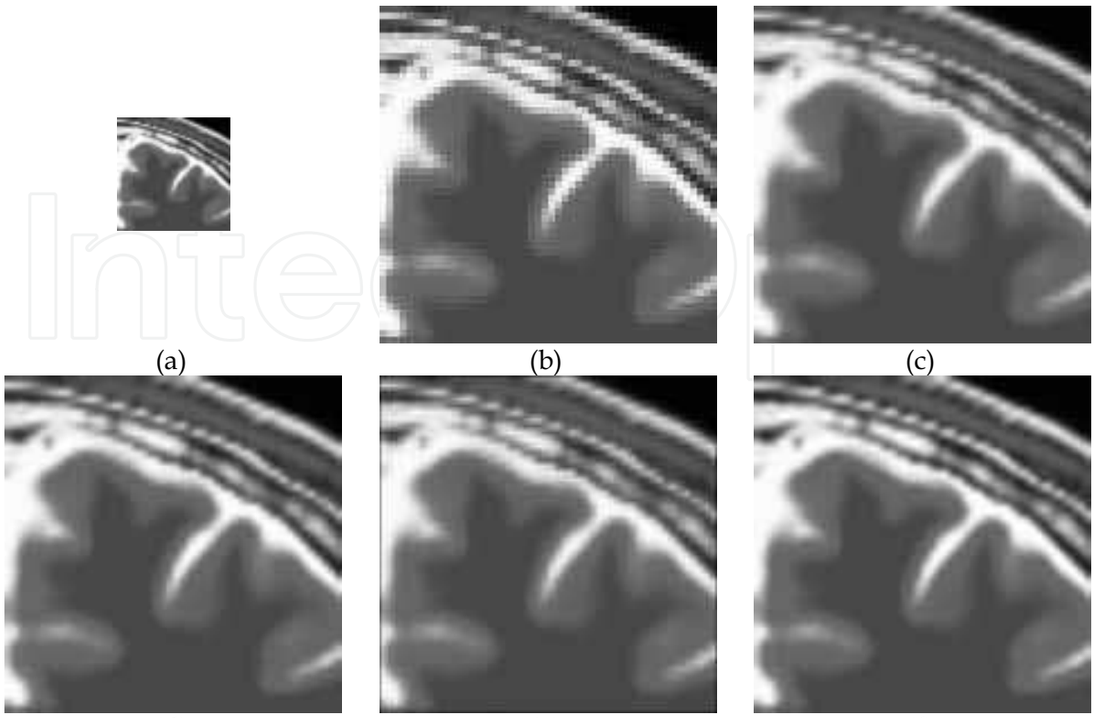

Fig. 16. Results with different interpolating kernels: original detail (a), 300% magnification with box-shaped kernel (b), triangular-shaped kernel (c), cubic kernel (d), gaussian kernel (e) and hamming sinc kernel (f).

Additionally, even if the subject goes beyond the purpose of this work, it is worth to remark that image resampling is not involved just in image reconstruction, but is also a critical matter in area-based registration techniques based on maximization of some similarity function. The choice of the interpolation method has relevant influence on the shape of such function, so a proper interpolation technique must be chosen to avoid the formation of local minima in the curve to optimize. In turn, such technique can be different from the one that provides us with the best visual results. For further reading on this topic, an interesting analysis was conducted by Liang et al. (2003).

5. Conclusion and future works

Image registration has become a fundamental pre-processing step for a large variety of modern medicine imaging tasks useful to support the experts' diagnosis. It allows to fuse information provided by sequential or multi-modality acquisitions in order to gather useful knowledge about tissues and anatomical parts. It can be used to correct the acquisition distortion due to low quality equipments or involuntary movements.

Over the last years, the work by a number of research groups has introduced a wide variety of methods for image registration. The problem to find the transformation function that best maps the input dataset onto the target one has been addressed by a large variety of

techniques which span from feature-based to area-based approaches depending on the amount of information used in the process.

A new framework for image registration has been introduced. It relies on kernel-based regression technique, using fuzzy membership functions as equivalent kernels. Such framework is presented in a formal fashion, which arises from the application and extension of the *Nadaraya-Watson* model.

The theoretic core has then been applied to two different landmark-based elastic registration schemes. The former simply predicts the pixels displacement after constructing the regression function starting from the known displacements of the landmarks. The latter, after a space subdivision of the dataset into triangles, computes the affine transformations that maps each triangle into the input image onto its correspondent in the target image. Such affine transformations are then composed to create a deformation surface, which exhibits crisp edges at the triangles junctions. In this case the regression function acts as a smoother for such surfaces; each point displacement is conditioned by the influence of the affine transformations of every surrounding zone of the image, receiving a larger contribute from closer areas.

Both the proposed registration algorithms have been extensively tested and some of the results have been reported. Comparisons with thin-plate spline literature method show that quality performances are generally better. At the same time timing performance is improved due to the absence of any optimization processes. The only drawback with the proposed methods is the size of the displacement function descriptor, which is bigger than TPS parameters vector, even though it keeps linear in the number of used landmarks.

Additional analysis were conducted on the resampling process involved in image registration. Several interpolation kernels have been described and analyzed.

As future work it is possible to extend the application of this framework towards a fully automatic area based registration with no needs of setting landmark points. For this purpose, new interpolation techniques will be designed to keep into account both image reconstruction quality and suppression of local minima in the optimization function.

According to the point-wise nature of these methods, it is possible to exploit the possibilities given by parallel computing, in particular with the use of GPU cluster-enhanced algorithms which will dramatically improve the process performance.

6. References

Ardizzone E., Gallea R, Gambino O. and Pirrone R. (2009). Fuzzy C-Means Inspired Free Form Deformation Technique for Registration. *WILF, International Workshop on Fuzzy Logic and Applications*. 2009.

Ardizzone E., Gallea R, Gambino O. and Pirrone R. (2009). Fuzzy Smoothed Composition of Local Mapping Transformations for Non-Rigid Image Registration. *ICIAP, International Conference on Image Analysis and Processing*. 2009

Bajcsy R., Kovacic S. (1989). Multiresolution elastic matching. *Computer Vision, Graphics, and Image Processing*, Vol. 46, No. 1. (April 1989), pp. 1-21.

Bezdek J. C. (1981): Pattern Recognition with Fuzzy Objective Function Algoritms, Plenum Press, New York.

Bookstein F.L. (1989). Principal Warps: Thin-Plate Splines and the Decomposition of Deformations, *IEEE Transactions on Pattern Analysis and Machine Intelligence*, vol. 11, no. 6, pp. 567-585, June, 1989.

Bro-Nielsen, M., Gramkow, C. (1996). Fast Fluid Registration of Medical Images. *Proceedings of the 4th international Conference on Visualization in Biomedical Computing* (September 22 - 25, 1996). K. H. Höhne and R. Kikinis, Eds. Lecture Notes In Computer Science, vol. 1131. Springer-Verlag, London, 267-276.

Cocosco C.A. , Kollokian V., Kwan R.K.-S.,Evans A.C. (1997). BrainWeb: Online Interface to a 3D MRI Simulated Brain Database. NeuroImage, vol.5, no.4, part 2/4, S425, 1997 -- *Proceedings of 3-rd International Conference on Functional Mapping of the Human Brain*, Copenhagen, May 1997.

Collins D.L., Zijdenbos A.P., Kollokian V., Sled J.G., Kabani N.J., Holmes C.J., Evans A.C. (1998). Design and Construction of a Realistic Digital Brain Phantom. *IEEE Transactions on Medical Imaging*, vol.17, No.3, p.463--468, June 1998.

Delaunay B.N. (1934). Sur la sph`ere vide. Bulletin of Academy of Sciences of the USSR, (6):793–800, 1934.

Dunn J. C. (1973). A Fuzzy Relative of the ISODATA Process and Its Use in Detecting Compact Well-Separated Clusters, *Journal of Cybernetics* 3: 32-57.

Fornefett M., Rohr K., Stiehl H.S. (1999). Elastic Registration of Medical Images Using Radial Basis Functions with Compact Support, *Computer Vision and Pattern Recognition, IEEE Computer Society Conference on*, vol. 1, pp. 1402, 1999 IEEE Computer Society Conference on Computer Vision and Pattern Recognition (CVPR'99) - Volume 1.

Kwan R.K.-S., Evans A.C., Pike G.B. (1996). An Extensible MRI Simulator for Post-Processing Evaluation. *Visualization in Biomedical Computing (VBC'96). Lecture Notes in Computer Science*, vol. 1131. Springer-Verlag, 1996. 135-140.

Kwan R.K.-S., Evans A.C., Pike G.B. (1999). MRI simulation-based evaluation of image-processing and classification methods. *IEEE Transactions on Medical Imaging*. 18(11):1085-97, Nov 1999.

Liang Z.P., Ji, J.X and Pan, H. (2003). Further analysis of interpolation effects in mutual information-based image registration, *Medical Imaging, IEEE Transactions on*, vol.22, no. 9, pp. 1131-1140, Sept. 2003

Nadaraya E. (1964). On estimating regression, Theory of Prob. and Appl., vol. 9, pp. 141–142, 1964.

Simon K.W. (1975), Digital image reconstruction and resampling for geometric manipulation, *Proceedings of IEEE Symposium on Machine Processing of Remotely Sensed Data*, 1975, pp. 3A-1–3A-11.

Wang Z., Bovik A.C., Sheikh H.R., Simoncelli E.P. (2004). Image quality assessment: From error visibility to structural similarity. *IEEE Transactions on Image Processing*, 13:600–612, 2004.

Watson G.S. (1964). Smooth regression analysis, Sankhya, Series A, vol. 26, pp. 359 – 372, 1964.

Wendland H. (1995). Piecewise polynomial, positive definite and compactly supported radial functions of minimal degree. Adv. Comput. Math. 4, p. 389.

Biomedical Engineering

Edited by Carlos Alexandre Barros de Mello

ISBN 978-953-307-013-1

Hard cover, 658 pages

Publisher InTech

Published online 01, October, 2009

Published in print edition October, 2009

Biomedical Engineering can be seen as a mix of Medicine, Engineering and Science. In fact, this is a natural connection, as the most complicated engineering masterpiece is the human body. And it is exactly to help our “body machine” that Biomedical Engineering has its niche. This book brings the state-of-the-art of some of the most important current research related to Biomedical Engineering. I am very honored to be editing such a valuable book, which has contributions of a selected group of researchers describing the best of their work. Through its 36 chapters, the reader will have access to works related to ECG, image processing, sensors, artificial intelligence, and several other exciting fields.

InTech Europe
University Campus STeP Ri
Slavka Krautzeka 83/A
51000 Rijeka, Croatia
Phone: +385 (51) 770 447
Fax: +385 (51) 686 166
www.intechopen.com

InTech China
Unit 405, Office Block, Hotel Equatorial Shanghai
No.65, Yan An Road (West), Shanghai, 200040, China
中国上海市延安西路65号上海国际贵都大饭店办公楼405单元
Phone: +86-21-62489820
Fax: +86-21-62489821

IntechOpen